Technical Paper

ISSN 1997-1400 Int. J. Pavement Res. Technol. 7(1):9-17

Stiffness Prediction of Recycled Aged CRM Binders Using an Artificial Neural Network

Yoo-Jae Kim[1], Ashley Kotwal[1], Hyunhwan Kim[1], and Soon-Jae Lee[1+]

Abstract: This research explores the utilization of an artificial neural network (ANN) in predicting the stiffness of recycled aged binders containing crumb rubber modifier (CRM). The data were organized into six independent variables (rotational viscosity of unaged, high failure temperatures of unaged and RTFO (rolling thin film oven) residual, and large molecular sizes of unaged, RTFO residual, and RTFO+PAV (pressure aging vessel) residual) covering the binder properties and one dependent variable, the binder stiffness. The training and testing results showed that the model explains 0.943 of the variability in stiffness, indicating that the ANN techniques are effective in predicting the stiffness of recycled aged CRM binders tested in this study.

DOI:10.6135/ijprt.org.tw/2014.7(1).9

Key words*: Artificial neural network; Crumb rubber modifier; Large molecular size; Stiffness.*

Introduction

More than 300 million scrap tires are disposed of in the United States every year. Approximately 67% of these are currently utilized for applications such as tire-derived fuel, molded products, and crumb rubber [1-3]. There is an increasing interest in using crumb rubber modified (CRM) binders in hot mix asphalt (HMA) pavements in the Unites States as well as in other countries [3-5]. This motivation was supported by previous studies reporting that CRM binders can produce asphalt pavements that exhibit increased pavement life, decreased traffic noise, reduced maintenance costs and resistance to rutting and cracking [2, 6-8].

Using CRM to modify asphalt binders in pavement engineering began more than four decades ago in the United States. The recycling of rubberized asphalt pavement is a very important issue because many of these pavements were constructed over 10-20 years ago, and some of them may now be candidates for recycling. Research on the recycling of rubberized asphalt concrete (RAC), conducted primarily by some state departments of transportation (DOTs) [9-12], has focused on investigating the in-field paving properties regarding the feasibility of recycling rubber-modified paving materials. The majority of a limited number of studies on the use of reclaimed rubberized materials in recycled asphalt paving mixtures indicate that these reclaimed materials can be successfully incorporated into other bituminous paving mixes [13]. Particularly for long-term performance characterizations, however, it is important to be able to identify the stiffness properties of rubberized binders to predict the long-term performance of these mixtures.

This study explores the feasibility of using a multilayer feed-forward artificial neural network (ANN) to predict the stiffness of recycled aged CRM binders. The CRM binders were artificially aged using rolling thin film oven (RTFO) + pressure aging oven (PAV) aging procedures, while the aged CRM binders were recycled using two base binders. The recycled aged CRM binders were artificially aged using the same RTFO+PAV methods. The gel permeation chromatography (GPC) parameters of unaged, RTFO residual, and RTFO+PAV residual were evaluated, and the Superpave binder properties were also measured at each aging state.

Materials

Asphalt Binders

Three performance grade (PG) 64-22 asphalt binders designated as A, B, and C from different crude sources were used in this study. Binder A was from a Venezuelan crude source, binder B was from a Middle Eastern source, and binder C was a mixture of several sources that could not be identified by the supplier. Table 1 shows the properties of three base binders.

Crumb Rubber Modifier (CRM)

The CRM produced by mechanical shredding at an ambient temperature was obtained from one source: -40 mesh (0.425 mm) and used with a gradation as shown as Fig. 1. To ensure that the consistency of the CRM was maintained throughout the study, only one batch of crumb rubber was used in this study.

CRM Binder Production and Aging

The CRM binder was produced in the laboratory at 177°C for 30 minutes by an open blade mixer at a blending speed of 700 rpm [14]. The percentage of crumb rubber added to the CRM binder was 10% by weight of the base binder. This mixing condition matches the practices used in South Carolina to produce field mixtures. The CRM binders were then artificially aged through a series of accelerated aging processes (RTFO aging for 85 minutes at 163°C and PAV aging for 20 hours at 100°C) [15].

Recycling of Aged CRM Binders

[1] Texas State University, San Marcos, TX 78666, U.S.A.

[+] Corresponding Author: E-mail soonjae93@gmail.com

Note: Submitted August 23, 2012; Revised April 2, 2013; Accepted June 10, 2013.

Table 1. Properties of Three Base Binders (PG 64-22).

Aging States	Test Properties	Binder Sources		
		A	B	C
Unaged Binder	Viscosity @ 135 °C (Pa-s)	0.405	0.626	0.457
	G*/sin δ @ 64 °C (kPa)	1.24	1.99	1.12
	Failure Temperature, °C	65.8	69.7	64.9
RTFO Aged Residual	G*/sin δ @ 64 °C (kPa)	3.3	6.09	2.53
	Failure Temperature, °C	67	72	65.1
RTFO + PAV Aged Residual	G*sin δ @ 25 °C (kPa)	2970	2420	1704
	Stiffness @ -12 °C (MPa)	183	129	117

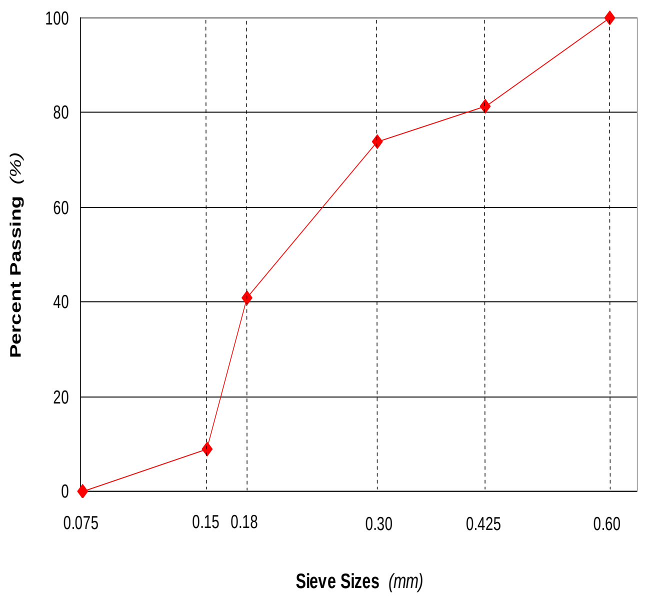

Fig. 1. Gradation of CRM Used in this Study.

Virgin CRM binders produced using the base binders of PG 64-22 were used for the recycling of 0% and 15% recycled binders. With respect to 25% and 35% recycled binders, the base binders of PG 58-22 were utilized to produce virgin CRM binders for the recycling. The recycled aged CRM binders were then artificially aged through RTFO and PAV processes. In total, thirty-six CRM binders (3 binder sources * 4 recycled binder percentages: 0%, 15%, 25%, and 35% * 3 aging levels: unaged, short-term aging, and long-term aging) were produced and evaluated during this study.

Superpave Binder Tests

The properties of these CRM binders were evaluated using selected Superpave binder test procedures including the viscosity test (AASHTO T 316), the bending beam rheometer (BBR) test (AASHTO T 313), and the dynamic shear rheometer (DSR) test (AASHTO T 315: with the plate gap adjusted to 2 mm). The plate gap adjustment was used to eliminate the influence of rubber particle size [16-18].

A 10.5 g binder sample of the binders was tested with a number 27 spindle in the rotational viscometer at 135 °C. In the DSR test, the binders (RTFO+PAV residual) were tested using an 8 mm parallel plate at 25 °C. The BBR test was conducted using each asphalt beam (125 × 6.35 × 12.7 mm) at -12 °C, and creep stiffness (S) and creep rate (m) of the binders were measured at a loading time of 60 s.

Gel Permeation Chromatography (GPC)

Waters GPC equipment with computerized software was used for the chromatographic analysis of binders. A differential refractive index meter (Waters 410) was used as a detector. For testing the samples at a constant temperature, the columns were kept at 35°C throughout the test in a column oven. The mobile phase was tetrahydrofuran (THF) flowing at a rate of 1 ml/min. The concentration rate used was 0.5% by weight of binder. This rate was recommended by the manufacturer of the equipment. Each GPC sample dissolved into THF was filtered through a 0.45μm syringe filter prior to injection into the injection module. A 50μl of dissolved sample was injected into the GPC injector for each test. Testing for each sample was repeated three times, then the average value of large molecular size (LMS) was reported.

Artificial Neural Network (ANN)

The artificial neural network (ANN) is a computational structure inspired by the architecture of biological neurons such as that of the human brain. The ANN is an interconnection of nodes, analogous to neurons. Each neural network has three critical components: node character, network topology and learning rules [19]. Node character determines how signals are processed by the node, such as the number of inputs and outputs associated with the node, the weight associated with each input and output, and the activation function. Network topology determines the ways in which nodes are organized and connected. Learning rules determine how the weights are initialized and adjusted.

The basic model for a node in the ANN is shown in Fig. 2. Each node receives multiple inputs from others via connections that have associated weight (w_i), analogous to the strength of the synapse. When the weighted sum of inputs exceed the threshold value of the node, it activates and passes the signal through a transfer function and sends it to neighboring nodes.

Multi Layer Perceptron (MLP)

The main type of ANN used in this study is referred to as a feed-forward network, which is called a multilayer perceptron [20]. The earliest type of the neural network is a single hidden-layer

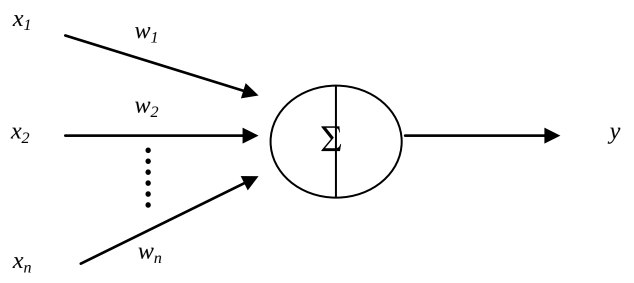

Fig. 2. A Typical Model of a Single Node.

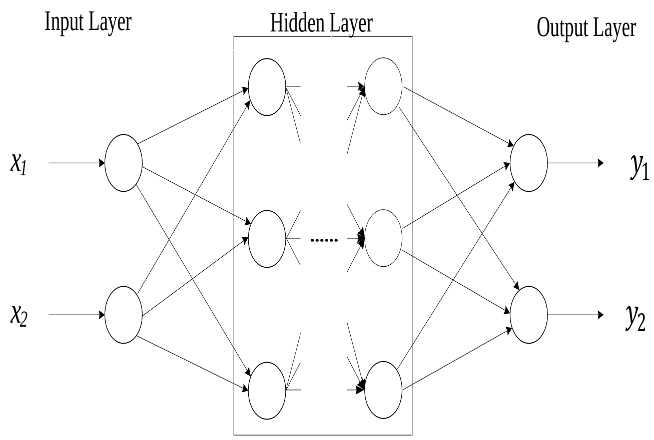

Fig. 3. Multilayer Perceptron.

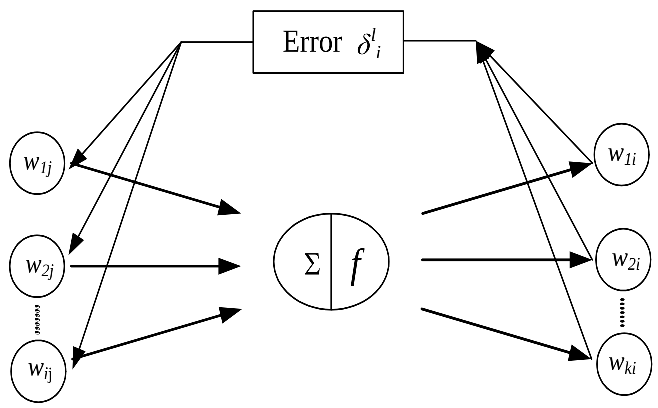

Fig. 4. Concept of a Back-Propagation.

perceptron that can solve only linearly separable problems. The multiple-layer perceptron (MLP) is the most widely used neural network shown in Fig. 3. It has one input layer, one output layer, and constructed neurons, as known processing elements named as hidden layers. The hidden layers are placed between the input and output layers. The processing elements in these hidden layers allow the network to represent and compute more complicated associations between input and output patterns. Each processing element receives a signal from the processing elements in the previous layer, and each of those signals is multiplied by a separate weight value. The weighted inputs are summed, then passed through a limiting function which scales the output to a fixed range of values. The output of the limiter is then broadcast to all of the processing elements in the next layer. The network operation consists of a highly nonlinear functional mapping of the processing elements in the hidden layers between the input and output variables. Hecht-Nielsen proved that a MLP could implement any function defined over a compact subset of Euclidean space [21].

Back-Propagation Algorithm

A back-propagation algorithm, also known as the generalized delta rule and chain rule, is the most commonly used learning rule and usually used in the training of MLP in areas such as speech and natural language processing, pattern recognition and system modeling. In the algorithm, the input is first propagated through the network, then the output is calculated. The error between the calculated output and the correct output, called the cost function, is then propagated backward from the output to the input to adjust the weights known as error back-propagation, or the generalized delta rule. The algorithm basically performs a gradient-descent method to minimize the mean square error cost function of all patterns presented during training. A typical back-propagation neural network architecture used in this paper is depicted in Fig. 4. The multilayer back-propagation ANN algorithm is used in this study.

Validation of the ANN Model

The evaluation of results is conducted using two indices: mean square error and correlation coefficient. The most widely utilized performance criterion to check the validation of the network is the average sum of square error known as mean square error (MSE) in the perceptron learning rule. Like least squares, the sum-of-squared errors is calculated by looking at the squared difference between what the network predicts for each training pattern and the target value, or observed value, for that pattern.

The other important performance criterion is the correlation coefficient (*r*). It is a quantity that gives the quality of the least squares fitting to the original data. The size of the mean square error (MSE) can be used to determine which line best fits the data, although it doesn't necessarily reflect whether a line fits the data tightly because the MSE depends on the magnitude of the data samples [22]. The correlation coefficient (*r*) solves this problem.

Modeling with ANN

A feed-forward back-propagation ANN model developed in this study used six variables (LMS of RTFO+ PAV residual, LMS of RTFO Residual, LMS of unaged binder, high failure temperature of RTFO residual, high failure temperature of unaged binder, and rotational viscosity of unaged binder) in the input layer, and one neuron in the output layer as illustrated in Fig. 5. One of the important issues in neural network is to appropriately set the number of hidden neurons. Experimentation must be conducted with the number of hidden-layer neurons and how it affects the output and learning dynamics of the network. The exact number of hidden layers and neurons and their connectivity must be specified before the network testing. The number of hidden neurons is usually determined via a trial procedure.

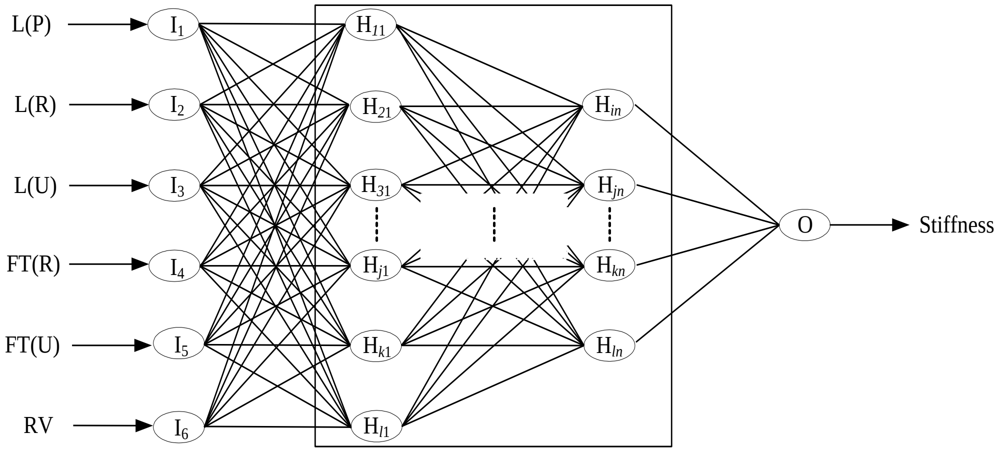

Fig. 5. Proposed NN Model.
L(P)=LMS of RTFO+PAV residual, L(R)=LMS of RTFO residual, L(U)=LMS of unaged, FT(R)=failure temperature of RTFO residual, FT(U)=failure temperature of unaged, and RV=rotational viscosity of unaged

Seven different neural network models were trained to find an optimum network architecture for the ANN model. The optimum architecture was chosen based on the minimum MSE and correlation coefficient by using cross validation to generate the model on different combinations of the input data set (Table 2) as obtained from the results of both the training and testing data sets in predicting the stiffness. Cross validation was used to train, test and validate the models due to the availability of the small number of data sets. The cross-validation is a method of estimating the accuracy of a prediction or regression model in which the input data set is divided into two parts, with each part in turn used to test a model fitted to the remaining parts. The trained ANN model is validated with the low testing MSE and Correlation Coefficient as compared to the training MSE and Correlation Coefficient value.

Results and Discussion

Superpave Binder Tests

The viscosity of the CRM binders with 15% recycled binder was the highest and that of the CRM binders with 25% recycled binder was lowest for all binder sources. For all three binder sources, CRM binder with 15% recycled binder resulted in the highest failure temperature, followed by CRM binder with 35% recycled binder. With respect to 25% recycled binder, using softer grade of PG 58-22 as a virgin binder, the CRM binder from binder sources A and B showed the lowest failure temperature within the same source.

After the RTFO aging procedure, the general trend was similar to the findings for high failure temperature at the original state. The CRM binder with 15% recycled binder showed the highest failure temperature within each binder source. After RTFO and PAV procedures, the stiffness of all recycled CRM binders was much less than 300 MPa, the maximum value for Superpave binder. Similar to the DSR test results at 25°C, the stiffness values from the BBR tests showed a similar trend regardless of the binder source.

GPC

Fig. 6 shows the average and standard deviation values of LMS (%) obtained from the three replicate samples of each recycled aged CRM binder, which included three aging states: original (unaged), RTFO residual, and RTFO+PAV residual. As expected, higher LMS values were caused by RTFO+PAV aging procedures, followed by RTFO aging procedure. This finding was true for all recycled aged CRM binders; regardless of the binder source and the RAP binder percentage. With respect to the RAP binder percentage, a general trend was found that the LMS value of the recycled aged CRM binders with 15% RAP binder was the highest at each aging state, and that of the CRM binders with 25% RAP binder was lowest at RTFO+PAV aging state for all binder sources. The difference in the LMS values are thought to be attributed to the use of different virgin binder grades (PG 64-22 for 15% RAP binder and PG 58-22 for 25% RAP binder). Based on the LMS values, the CRM binders with the highest RAP binder percentage of 35% were found to have generally softer binder properties than those with 15% RAP binder.

ANN

The stiffness of an asphalt binder is extremely important in determining how well a pavement performs and is fundamental in the analysis of response to traffic loads. The stiffness of recycled aged binders containing CRM is influenced by several parameters: the aging and recycling properties of rubberized binders, molecular size of binders, viscosity and failure temperature. Therefore, characterizing recycled aged CRM binders requires an extensive understanding of the relation between these parameters and the properties of the resulting matrix. The input for recycled aged CRM binders has been chosen as L(P) = LMS of RTFO+PAV residual, L(R) = LMS of RTFO Residual, L(U) = LMS of unaged, FT(R) = Failure temperature of RTFO residual, FT(U) = Failure temperature of unaged, and RV = Rotational viscosity of unaged, with the output being the stiffness of recycled aged CRM binder [5].

To architect a steady ANN model based on the determined input number, the parametric study is conducted by changing the number of neurons in the hidden layers (one and two hidden layers) in order to test the stability of the network. From MSE and correlation

Table 2. The Examples of Collected Data Sets.

NO.	RV(Pa-s)	FT(UNAGED) (℃)	FT(RTFO) (℃)	STIFFNESS (MPa)	LMS(UNAGED) (%)	LMS(RTFO) (%)	LMS(PAV) (%)
1	1.212	72.1	77.8	55	13.47	16.94	20.85
2	1.263	71.7	77.3	51	14.05	16.68	20.95
3	0.938	71.9	77.1	52	13.21	17.35	21.74
4	2.375	81.8	86.3	132	15.59	19.28	23.91
5	2.237	80.9	85.8	133	15.57	19.14	24.13
6	2.375	81.4	86.5	121	15.89	19.69	24.05
7	2.45	86.3	85.9	138	17.5	21.12	25.3
8	2.537	85.6	86.7	147	17.6	20.9	24.73
9	2.575	86.6	86.7	137	16.64	20.75	24.48
10	2.101	79.8	81.7	76	16.11	19.5	21.98
11	2.152	79.5	82.8	76	16.07	19.32	22.94
12	1.998	79.6	81.8	76	16.14	19.73	23.68
13	2.412	83	83.5	82	16.69	21.67	24.28
14	2.409	83.6	83.1	87	17.46	21.61	23.81
15	2.307	83.6	83.9	84	17.38	20.45	24.75
16	0.6	66.9	65.6	59	13.72	17.28	21.85
17	0.588	66.9	66	59	13.47	17.19	21.47
18	0.675	66.8	66.1	58	13.28	17.39	22.39
19	1.288	72.4	72.8	144	16.29	19.78	25.92
20	1.375	73.6	72.9	145	16.65	19.58	24.98
21	1.2	72.8	72.4	154	15.77	19.96	25.51
22	1.413	77.2	74.9	149	17.58	21.41	26.05
23	1.362	77.2	74.7	155	17.7	21.64	26.01
24	1.362	77.1	74.8	151	17.85	21.69	26.14
25	0.975	71.5	71.4	83	15.28	17.74	24.42
26	1.075	70.8	71.2	78	15.26	18.51	23.89
27	1.125	71	71.9	81	15.32	18.31	23.84
28	1.138	73.5	72	96	16.27	19.95	24.95
29	1.188	74.4	71.6	90	16.47	20.15	24.58
30	1.337	74.2	72.4	93	16.78	20.57	25.27
31	0.713	69	70.4	86	13.28	17.42	19.17
32	0.775	68.1	70.9	86	12.74	17.45	20.68
33	0.825	68.6	70.5	87	13.19	17.41	20.54
34	1.257	73.4	72.6	148	14.62	17.5	24.8
35	1.287	74.4	73	139	14.61	17.92	24.84
36	1.363	74	72.9	139	14.55	18.11	24.02
37	1.579	78.8	79.9	158	17.19	20.93	27.2
38	1.587	78.8	77.9	143	15.8	20.47	25.99
39	1.659	79.8	78.4	150	15.27	20.14	26.64
40	1.108	76.1	76	96	15.28	17.59	22.35
41	1.206	76.4	75.4	92	15.66	18.29	22.12
42	1.259	76.3	75.7	94	15.34	18.33	22.59
43	1.458	77.9	76.9	124	16.38	20.55	24.83
44	1.589	78.4	76.3	126	16.51	20.35	24.4
45	1.557	78	76.4	123	16.27	20.01	24.18

coefficients with different ANN configurations, the optimal number of hidden layers, as well as neurons in the hidden layer, were selected. The activation function in the hidden and output layers was chosen as a hyperbolic tangent sigmoid function. Other user-defined parameters used were momentum = 0.1 and learning rate = 0.1. The performance effects of the parameters, MSE and correlation coefficients were studied, and the values of the parameters are shown in Tables 3 and 4.

Table 3 shows the performance of the networks with various numbers of neurons in one hidden layer. The representation of the network is as follows in the model of 6-2-1: 6 input neurons, 2 neurons in hidden layer, and 1 output neuron, respectively. For the trained data, the correlation coefficients in all cases of the networks were found to be more than 0.97. Conversely, the testing correlation coefficients obtained for almost all cases were between 0.657 and 0.7440, while the 6-7-1 was observed at .948. The testing and training MSEs for the 6-2-1 through 6-6-1 and 6-8-1 resulted in nearly identical values (See Table 3). The training and testing MSEs

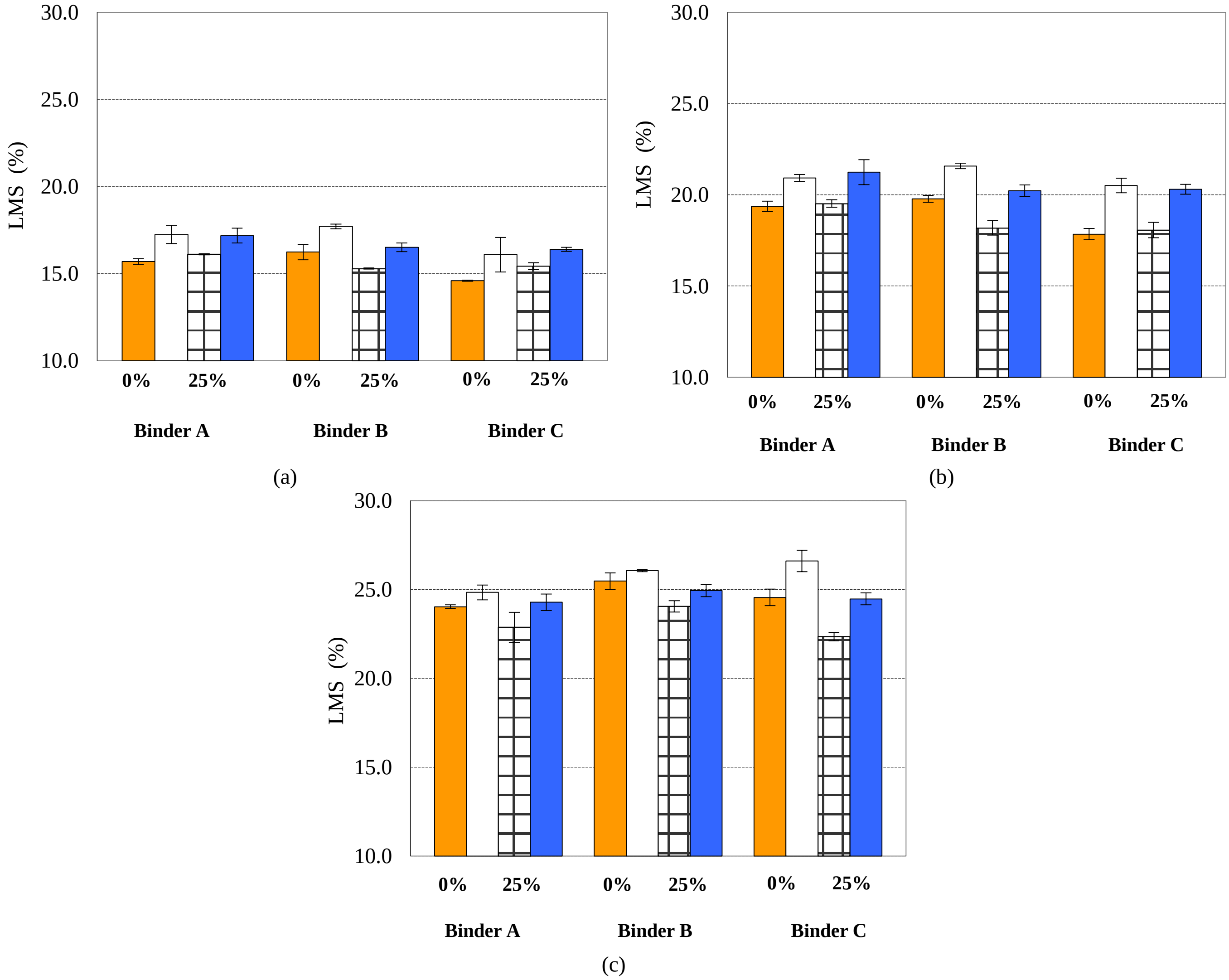

Fig. 6. LMS (%) of Recycled Aged CRM Binders: (a) Unaged; (b) RTFO Residual; and (c) RTFO+PAV Residual.

Table 3. Comparison of Mean Squared Error and Correlation Coefficient with One Hidden Layer

ANN Models	Training		Testing	
	MSE	Correlation Coefficient (*r*)	MSE	Correlation Coefficient (*r*)
6-2-1	0.0181	0.971	0.186	0.657
6-3-1	0.0134	0.979	0.162	0.714
6-4-1	0.0085	0.986	0.164	0.723
6-5-1	0.0086	0.986	0.150	0.744
6-6-1	0.0081	0.987	0.174	0.686
6-7-1	0.0069	0.989	0.036	0.948
6-8-1	0.0086	0.986	0.180	0.670

Table 4. Comparison of Mean Squared Error and Correlation Coefficient with Two Hidden Layers.

ANN Models	Training			Testing		
	MSE	Correlation Coefficient (*r*)	Error (%)	MSE	Correlation Coefficient (*r*)	Error (%)
6-7-3-1	0.0079	0.988	3.9	0.1859	0.667	23.5
6-7-4-1	0.0265	0.958	7.8	0.1047	0.839	16.1
6-7-5-1	0.0076	0.988	3.7	0.1615	0.707	21.6
6-7-6-1	0.0074	0.988	3.4	0.1730	0.680	22.0
6-7-7-1	0.0091	0.986	4.4	0.1732	0.686	22.7
6-7-8-1	0.0094	0.985	4.8	0.1769	0.690	23.1
6-7-9-1	0.0074	0.988	3.7	0.0393	0.943	7.5

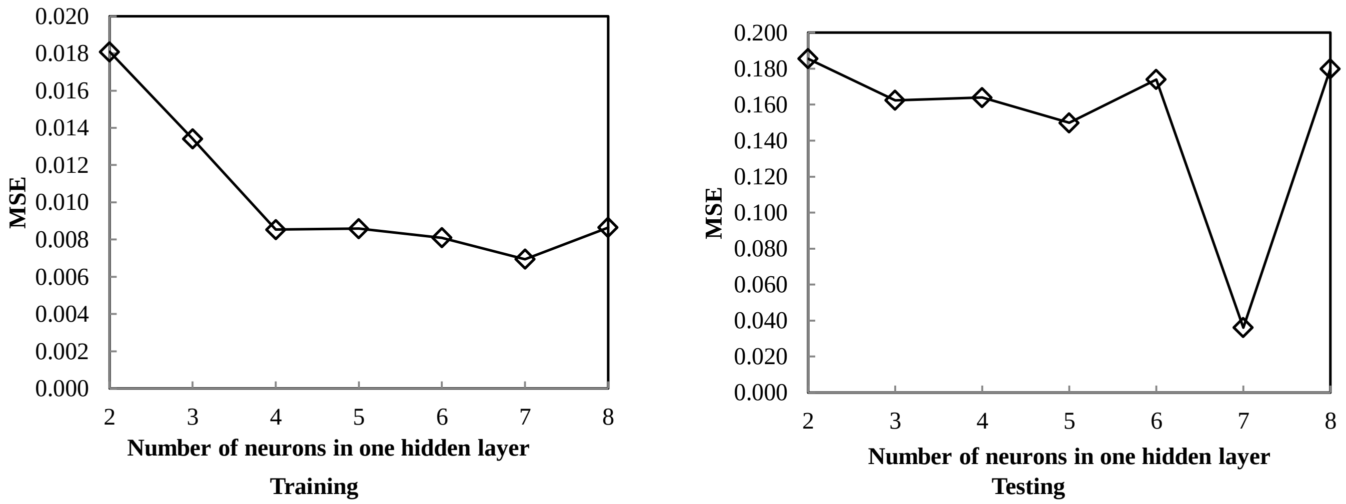

Fig. 7. Comparison of the Performance of Models for Training and Testing.

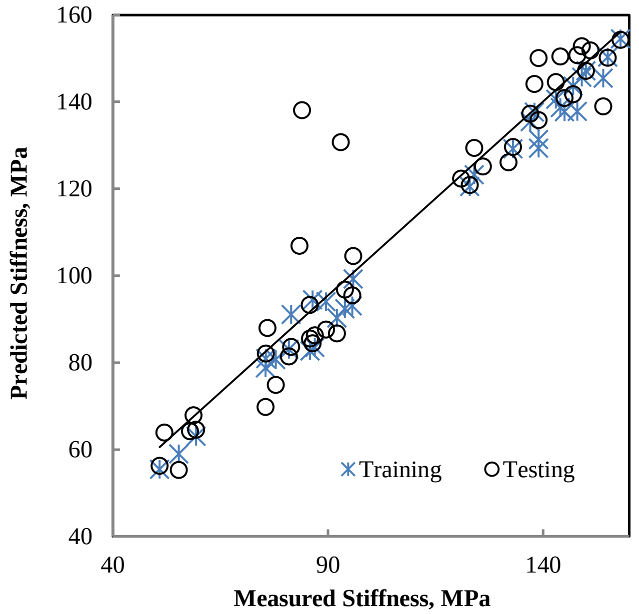

Fig. 8. Measured Versus Predicted Stiffness of Recycled Aged CRM Binders with ANN (6-7-9-1) Model.

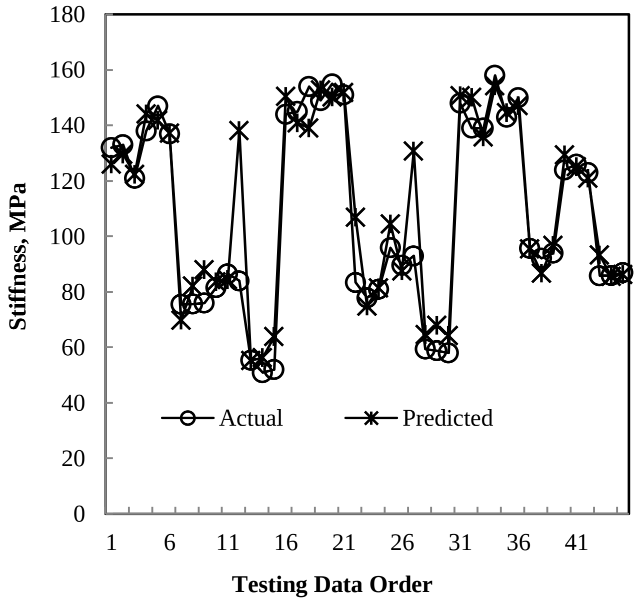

Fig. 9. Comparison of the Actual and Predicted Stiffness of Recycled Aged CRM Binders with ANN (6-7-9-1) Model.

were smallest for the 6-7-1, 0.0069 and 0.036, respectively.

Fig. 7 shows that the performance of the network with various numbers of neurons in one hidden layer is measured by the MSE. The MSE varied significantly for trained data, dependent on the number of neurons. Under tested data, however, the 6-2-1 to 6-6-1 and 6-8-1 indicated that the number of neurons does not appear to affect the MSE as much. The 6-7-1 has the lowest MSE and highest correlation coefficient with measured results for both training and testing sets. A further test on whether an additional second hidden layer could improve the network performance was conducted. In this test, the number of 7 neurons in the first hidden layer was fixed and various numbers of neurons in the second layer were evaluated.

Table 4 shows the MSEs and correlation coefficients obtained from the seven networks, with a various number of neurons in two hidden layers. The 6-7-3-1 (6 input neurons, 7 and 3 neurons in hidden layers, and 1 output neuron, respectively), 6-7-7-1, and 6-7-8-1 did not benefit significantly from the training process because of their limited capacity to perform nonlinear mapping of the input variables. The higher value of correlation coefficients and a smaller value MSE result in improved performance of the model. The training MSEs and correlation coefficients for the 6-7-3-1, 6-7-5-1, 6-7-6-1 and 6-7-9-1 combination were nearly identical. The 6-7-9-1 was chosen as the optimum model for the ANN model based on its low training and testing MSE and correlation coefficient. The 6-7-9-1 trained network was used to run a set of test data.

Fig. 8 and 9 represent the scatter diagrams of measured and predicted values of stiffness from trained and tested data. The prediction is fairly close to the corresponding measured values of stiffness. For trained data, it was observed that a MSE of 0.0074, correlation coefficient of 0.988, and mean absolute error of 3.7% were obtained. Also, for testing data, it was observed that a MSE of 0.0393, correlation coefficient of 0.943, and mean absolute error of 7.5% were obtained. The results for stiffness of recycled aged CRM binders indicate that the model as fitted accounts for 0.943 of the variability in stiffness with the 6-7-9-1 ANN model.

The important indices of six input variables show that the LMS of unaged (the learned weight of 0.7415), high failure temperature of unaged (0.7364), and rotational viscosity of unaged (0.6853) are the most important factors in the developed models to predict stiffness values for the recycled aged binders containing crumb rubber. However, LMS of RTFO residual, LMS of RTFO+PAV residual, and high failure temperature of RTFO residual are relatively unimportant as compared to the other independent variables.

Conclusions

The following conclusions were reached based on the limited experimental data presented regarding the stiffness of recycled aged CRM binders:

1. The laboratory-prepared recycled binders containing CRM were utilized up to 35%, and in most cases, the performance properties of recycled aged CRM binders showed the results meeting current Superpave binder requirements.
2. The RTFO and RTFO+PAV aging procedures resulted in a gradual increase in the LMS values for recycled aged CRM binders. In general, recycled aged CRM binders with 15% and 25% RAP binders showed the highest and lowest LMS values within each aging state, respectively.
3. The ANN model with six variables explained 0.943 of the variability in stiffness for the recycled aged CRM binder.
4. The stiffness was strongly dependent on the LMS of unaged binder.
5. The stiffness was weakly dependent on the high failure temperature of RTFO residual.
6. The ANN approach used in this study has been shown to be effective in creating a feasible predictive model. The established ANN-based models were able to predict the stiffness accurately.

References

1. Amirkhanian, S. and Corley, M. (2004). Utilization of Rubberized Asphalt in the United States—An Overview, *Proceedings of 04 International Symposium Advanced Technologies in Asphalt Pavements*, South Korea, pp. 3-13.
2. Feipeng, X., Amirkhanian, S., and Juang, C.H. (2009). Prediction of Fatigue Life or Rubberized Asphalt Concrete Mixtures Containing Reclaimed Asphalt Pavement Using Artificial Neural Networks, *Journal of Materials in Civil Engineering*, 21(6), pp. 253-261.
3. Shen, J., Amirkhanian, S., and Lee, S.-J. (2005). Effects of Rejuvenating Agents on Recycled Aged Rubber Modified Binders, *The International Journal of Pavement Engineering*, 6(4), pp. 273-279.
4. Bahia, H.U. and Davis, R. (1994). Effect of Crumb Rubber Modifiers (CRM) on Performance Related Properties of Asphalt Binders, *Journal of the Association of Asphalt Paving Technologists*, Vol. 63, pp. 414-449.
5. Lee, S.-J., Amirkhanian, S., and Putman, B. (2009). Characterization of Recycled Aged RAP Binders Containing Crumb Rubber Modifier Using Gel Permeation Chromatography, *Journal of Materials in Civil Engineering*, 21(8), pp. 382-391.
6. Huang, B., Mohammad, L.N., Graves, P.S., and Abadie, C. (2002). Louisiana Experience with Crumb Rubber-Modified Hot-Mix Asphalt Pavement, *Transportation Research Record*, No. 1789, pp. 1-13.
7. Liang, R.Y. and Lee, S. (1996). Short-Term and Long-Term Aging Behavior of Rubber Modified Asphalt Paving Mixtures, *Transportation Research Record*, No. 1530, pp. 11-17.
8. Ruth, B.E. and Roque, R. (1995). Crumb Rubber Modifier (CRM) in Asphalt Pavements, *Proceedings of the Transportation Congress*, pp. 768-785, San Diego, California, USA.
9. Albritton, G.E., Barstis, W.F. and Gatlin, G.R. (1999). Construction and Testing of Crumb Rubber Modified Hot Mix Asphalt Pavement, *Report No: FHWA/MS-DOT-RD-99-115*, Federal Highway Administration, Washington, D.C., USA.
10. Bischoff, D. and Toepel, A. (2004). *Tire Rubber in Hot Mix Asphalt Pavement*, Wisconsin Department of Transportation, Madison, Wisconsin, USA.
11. Crockford, W.W., Makunike, D., Davison, R.R., Scullion, T. and Billiter, T.C. (1995). Recycling Crumb Rubber Modified Pavements, *Texas Transportation Institute Research Report 1333-1F*, Texas A&M University, College Station, Texas, USA.
12. Gunkel, K.O'C. (1994). *Evaluation of Exhaust Gas Emissions and Worker Exposure from Asphalt-Rubber Binders in Hot Mix Asphalt Mixtures Part I: Exhaust Gas Emissions Results*, Wildwood Environmental Engineering Consultants, Inc. for Michigan Department of Transportation, USA.
13. Caltrans. (2005). *Feasibility of Recycling Rubber-Modified Paving Materials*, Materials Engineering and Testing Services, Office of Flexible Pavement Materials, Caltrans, Sacramento, California, USA.
14. Shen, J., Amirkhanian, S., Xiao, F. (2006). High-Pressure Gel Permeation Chromatography of Aging of Recycled Crumb Rubber-Modified Binders with Rejuvenating Agents, *Transportation Research Record*, No. 1962, pp. 21-27.
15. The Asphalt Institute. (2003). *Performance Graded Asphalt Binder Specification and Testing, SP-1*. The Asphalt Institute, Lexington, Kentucky, USA.
16. Heitzman, M. (1992). Design and Construction of Asphalt Paving Materials with Crumb Rubber Modifier, *Transportation Research Record*, No. 1339, pp. 1-8.
17. Kim, S., Loh, S.W., Zhai, H. and Bahia, H. (2001). Advanced Characterization of Crumb Rubber-Modified Asphalts, Using Protocols Developed for Complex Binder, *Transportation Research Record*, No. 1767, pp. 15-24.
18. Zanzotto, L. and Kennepohl, G. (1996). Development of Rubber and Asphalt Binders by Depolymerization and Devulcanization of Scrap Tires in Asphalt, *Transportation Research Record*, No. 1530, pp. 51-59.

19. Livingstone, D. J. (2008). *Artificial Neural Network Methods and Applications*, Humana Press, Sandown, UK.
20. Rosenblatt, F. (1962). *Principles of Neurodynamics: Perceptrons and the Theory of Brain Mechanisms*, Spartan New York, USA.
21. Hecht-Nielsen, R. (1991). Theory of the Black-Propagation Neural Network, *Neural Networks for Perception*. H. Wechsler Ed., pp. 65-93, Academic Press, San Diego, California, USA.
22. Principe, N. R. (1999). *Neural and Adaptive Systems: Fundamentals through Simulation*, John Wiley & Sons, Inc., New York, New York, USA.